Available online at www.sciencedirect.com
SCIENCE DIRECT®
Chemical Physics 298 (2004) 119–123
Chemical Physics
www.elsevier.com/locate/chemphys

Effects of tertiary butyl substitution on the charge transporting properties of rubrene-based films

H.H. Fong [a], S.K. So [a,*], W.Y. Sham [b], C.F. Lo [b], Y.S. Wu [c], C.H. Chen [c]

[a] *Department of Physics and Center for Advanced Luminescence Materials, Hong Kong Baptist University, Kowloon Tong, Hong Kong, China*
[b] *Department of Physics, The Chinese University of Hong Kong, Shatin, N.T., Hong Kong, China*
[c] *Department of Applied Chemistry, Microelectronics and Information Systems Research Center, National Chiao Tung University, Hsinchu, Taiwan 300, ROC*

Received 6 October 2003; accepted 10 November 2003

Abstract

The charge transporting properties of rubrene (5,6,11,12-tetraphenylnaphthacene or RB), and a new rubrene-based complex, tetra(*t*-butyl)-rubrene [2,8-di(*t*-butyl)-5,11-di[4-(*t*-butyl)phenyl]-6,12-diphenylnaphthacene or TBRB], were examined in the form of amorphous films as functions of electric field and temperature by means of time-of-flight technique. At room temperature, the hole mobility μ for RB is $7–9 \times 10^{-3}$ $cm^2 V^{-1} s^{-1}$ whereas μ for the more bulky TBRB is about 2×10^{-3} $cm^2 V^{-1} s^{-1}$. The microscopic conduction mechanism in both materials can be modeled by the Gaussian disorder model in which hopping conduction occurs through a manifold of sites with energetic and positional disorder. The energetic disorder in RB and TBRB is almost identical and is about 78 meV in each case, and is mainly controlled by van der Waals interaction. The *t*-butyl groups in TBRB induce large fluctuations in the spatial separation among TBRB molecules and result in an increase in the positional disorder, and hence a reduction in the hole mobility.

Keywords: Rubrene; Hole mobility; Organic charge transporters

1. Introduction

Organic electronic materials are receiving widespread attention due to realization of emerging optoelectronic devices. Well-known examples are organic light-emitting diodes (OLEDs), solar cells, and thin film transistors [1–4]. In the case of OLEDs, much attention has been directed towards the search of stable and efficient light-emitting organic molecules. Among all common light-emitters, rubrene (5,6,11,12-tetraphenylnaphthacene or RB) is generally considered to be a very important dopant for yellow light emission [5]. RB emits with nearly unity quantum efficiency at diluted phase. When RB is doped into *tris* (8-hydroxyquinolinato) aluminum (Alq_3) or N,N'-bis-(1-naphthyl)-N,N'-diphenyl-1,1′-biphenyl-4,4′-diamine (NPB), efficient Förster energy transfer occurs [6]. RB, however, is also known to affect electrical transport in organic charge transporters. Previously, we have shown that N,N'-diphenyl-N,N'-bis(3-methylphenyl)-(1,1′-biphenyl)-4,4′-diamine (TPD) doped with rubrene has a lower hole mobility than undoped TPD [7]. As a result, OLEDs with RB-doped TPD as the hole-transporting layer has better charge balance, and improved device lifetime [4]. Another interesting aspect of RB is that all by itself, RB is a good charge transporter. In fact, it is known that in the crystalline state, RB exhibits a large hole mobility of a fraction of $cm^2 V^{-1} s^{-1}$ [8]. Yet, in amorphous form, the charge transport property of RB is not well-known.

The present study aims at studying the charge transporting properties of RB and a new rubrene-based complex, tetra(*t*-butyl)-rubrene [2,8-di(*t*-butyl)-5,11-di[4-(*t*-butyl)phenyl]-6,12-diphenylnaphthacene or TBRB], in amorphous states by time-of-flight (TOF) technique. The chemical structures of both molecules are shown in Fig. 1(a). TBRB is synthesized by attaching four tertiary butyl groups to RB. The physical properties of TBRB

* Corresponding author. Tel.: +85234115883; fax: +85234115813.
E-mail address: skso@hkbu.edu.hk (S.K. So).

0301-0104/$ - see front matter © 2003 Elsevier B.V. All rights reserved.
doi:10.1016/j.chemphys.2003.11.008

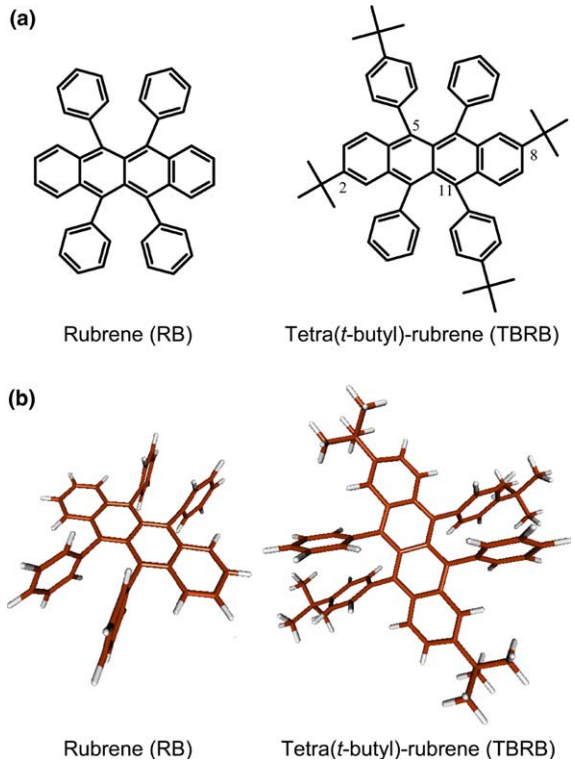

Fig. 1. (a) Molecular structures of RB and TBRB, and (b) the optimized ground state molecular structures of RB, and TBRB. The geometries of RB and TBRB are optimized by unrestricted HF/6-31G(d) method.

have been described elsewhere [9]. Briefly, the absorption and photoluminescence spectra of both RB and TBRB are very similar and so, the additional *t*-butyl groups do not have much influence on the optical properties of TBRB. However, TBRB is thermally more stable and more resistant to luminescence quenching than RB. Thus, TBRB exhibits better luminous efficiency (up to 5.6 cd/A) when used as a dopant in Alq_3-based OLEDs [9]. It is, therefore, interesting to use RB as a reference and to see how the carrier mobility will be affected by the presence of the *t*-butyl groups in TBRB. Furthermore, direct evaluation of their carrier mobilities and a sound understanding of their microscopic conductivity mechanism will shed light on the future design of new molecular charge transporting complexes for organic photonic devices.

2. Experimental

RB was purchased from Aldrich and was used without further purification. TBRB was synthesized following the literature described elsewhere [9]. Indium-tin-oxide (ITO) on glass (2.5 cm × 2.5 cm, 72 Ω/sq) was used as the substrate for the TOF samples. The substrate was solvent cleaned by standard procedures before sample fabrication [10]. All organic films were deposited by thermal evaporation under a base pressure of 10^{-6} Torr. The sample has a general structure of Al (15 nm)/TPD (30 nm)/*X*/ITO, where *X* is RB (6 μm) or TBRB (4 μm). TPD acts as a charge injection layer for holes. The coating rate for RB and TBRB was 19 Å/s while the rate for TPD was about 1 Å/s. The thicknesses of organic layers were monitored in situ with a quartz crystal sensor and further calibrated by a profilometer (Tencor Alpha-step 500). After coating, the sample was immediately loaded inside a cryostat for measurements. The sample temperature was regulated between 233 and 289 K. The crystallinity of RB or TBRB film was examined by X-ray diffraction (XRD) using a Rigaku Ru-200B D-MAX X-ray diffractometer. The XRD of evaporated RB and TBRB neat films were featureless, and hence the films were amorphous.

The schematic diagram of the TOF setup has been described in Ref. [7]. A nitrogen pulsed laser (Laser Science, Model VSL-337ND-S, $\lambda = 337.1$ nm, pulse duration = 4 ns) having a beam size of 28.3 mm^2 was used to generate photocarriers. The laser beam was directed from the semi-transparent Al side to create electron–hole pairs inside TPD layer. At 337.1 nm, TPD possesses an optical absorption coefficient of 1.8×10^5 cm^{-1}. The charges generated within this relatively thin layer (30 nm) can be presumed to be a sheet charge and provide abundant photocarriers for hole injection. The dwell time of holes in the TPD layer is negligible compared to the transit time of hole inside RB or TBRB. In addition, the highest occupied molecular orbital (HOMO) of TPD is about 5.6 eV, which is 0.1–0.2 eV higher than the HOMO of RB (5.38 eV) or TBRB (5.49 eV) [9]. So hole injection from the TPD layer to either RB or TBRB layer is barrier-free.

3. Results and discussion

Fig. 2(a) shows a typical time transient for the hole carriers in a RB film at 289 K. The film thickness *d* was 6 μm and the applied field *F* was 0.1 MV/cm. The TOF transient can be regarded as non-dispersive. The hole mobility μ was computed using the well-known relation: $\mu = d^2/(V \cdot \tau)$, where *V* is the applied voltage and τ is the flight time as determined from the inset of Fig. 2(a) [7]. Fig. 3(a) shows the field dependent mobility of RB from 233–289 K. The field dependence of hole mobility closely follows the Poole–Frenkel (PF) form, where $\mu \propto \exp(\beta\sqrt{F})$, *F* is the applied electric field, and β is a constant at a fixed temperature. At 289 K, the hole mobility is in the range of $7–9 \times 10^{-3}$ $cm^2\,V^{-1}\,s^{-1}$. The hole mobility for the amorphous RB film is higher than many common organic hole transporters in amorphous state. However, the hole mobility is substantially lower than that of crystalline RB (>1 $cm^2\,V^{-1}\,s^{-1}$) [8].

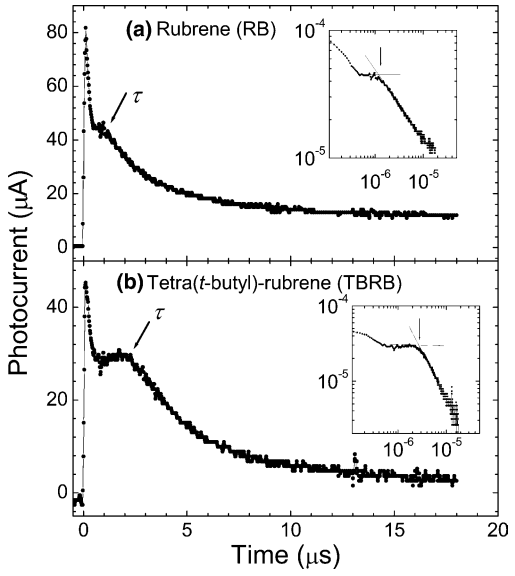

Fig. 2. Typical TOF transients for (a) RB under $F = 0.07$ MV/cm, and (b) TBRB under $F = 0.05$ MV/cm at 278 K where F is the external electric field across the sample. The insets show the time transients in log–log plots.

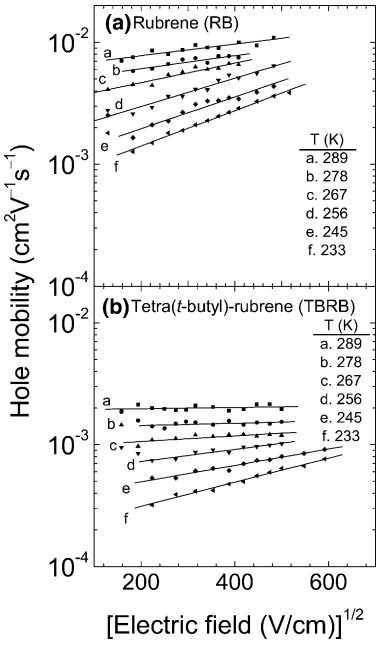

Fig. 3. Hole mobilities of (a) RB, and (b) TBRB at different temperatures vs. the square root of the applied field.

Fig. 2(b) shows the TOF transient at 289 K while Fig. 3(b) summarizes the field and the temperature dependence of the hole mobility of TBRB. The results are in excellent agreement with the PF dependence. The hole mobility for TBRB is generally lower than that of RB. Furthermore, for TBRB, the variation of μ with F is weaker than RB. At 289 K, the hole mobility is practically a constant with a value of 2×10^{-3} cm^2 V^{-1} s^{-1}.

The hole transporting behavior in many amorphous molecular solids can be modeled by the Gaussian disorder model (GDM) [11]. Molecules are regarded as uncorrelated localized hopping sites, whose site energies distribution is assumed to be Gaussian. In the GDM, charge transport by the means of hopping among these localized states subject to (a) built-in energetic disorder σ, and (b) positional disorder Σ. The hopping rate is characterized by Miller–Abrahams (MA) type, originally proposed to describe low temperature impurity hopping in semiconductor [12]. The energetic disorder can be treated as the width of the Gaussian density of states while the positional disorder can be understood as the spatial disorder or packing constraint. Under GDM, the carrier mobility can be described by the following equation:

$$\mu(F,T) = \mu_\infty \exp\left[-\left(\frac{2\sigma}{3kT}\right)^2\right] \exp\left[\beta\sqrt{F}\right], \qquad (1)$$

where T is the absolute temperature, k is the Boltzmann constant, $\beta = C[(\sigma/kT)^2 - \Sigma^2]$, μ_∞ is the high temperature limit of the mobility, and C is a constant. Eq. (1) predicts that hole mobilities of both RB and TBRB samples depend exponentially on $\sqrt{F}$ at fixed temperature. From Fig. 3, the mobilities of RB and TBRB follow this prediction very well. Furthermore, the mobility should depend exponentially on $-1/T^2$ when F vanishes. Fig. 4(a) and (b) depict the zero-field mobility $\mu(0,T)$ extrapolated for each temperature from Fig. 3 and reveal the linear dependence predicted by Eq. (1). From the slope of $\mu(0,T)$ vs. $1/T^2$ plot, the energetic disorder σ was found to be 0.077 eV for both RB and TBRB. The energetic disorder can be interpreted as the width of the HOMO of RB or TBRB.

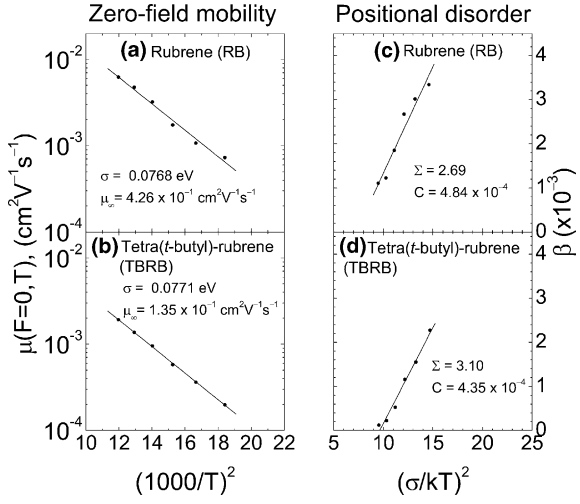

Fig. 4. The zero field mobilities vs. $1/T^2$ for (a) RB and (b) TBRB; the corresponding β vs. $1/T^2$ for (c) RB, and (d) TBRB. From these plots, the energetic and positional disorders can be extracted.

The positional disorder Σ for RB and TBRB can be obtained by plotting β against $(\sigma/kT)^2$ as shown in Fig. 4(c) and (d). The values of Σ were found to be 2.69 and 3.10 for RB and TBRB, respectively. The similarity of σ in RB and TBRB suggests that the *t*-butyl groups in TBRB have negligible effect in the energetic disorder. On the contrary, the *t*-butyl groups appear to have direct influence on the positional disorder, changing Σ from 2.69 to 3.10. In sum, within the framework of GDM, the mobility reduction in TBRB is due to the increase of the positional disorder associated with the *t*-butyl groups.

In order to obtain further insights into the transport behavior of RB and TBRB, the ground state geometries and frontier orbitals of these two molecules have been investigated computationally by ab initio calculations using the Gaussian 98 [13]. The ground state molecular structures were optimized at the unrestricted Hartree–Fock (HF) level with the 6-31G(d) basis set (UHF/6-31G(d)). Density functional theory (DFT) was then applied to compute the Kohn–Sham (KS) molecular orbitals, employing the B3LYP/6-31G(d) density functional. The computed structures are shown in Fig. 1(b). The naphthacene moiety in RB is essentially planar, whereas the naphthacene moiety in TBRB is twisted by about 44°. Fig. 5 shows in addition the frontier orbitals of RB and TBRB. The HOMOs and the lowest unoccupied molecular orbitals (LUMOs) of both molecules have very similar features. They are mainly localized on the naphthacene moieties. However, there is little contribution to the frontier orbitals from either the phenyl or *t*-butyl side groups.

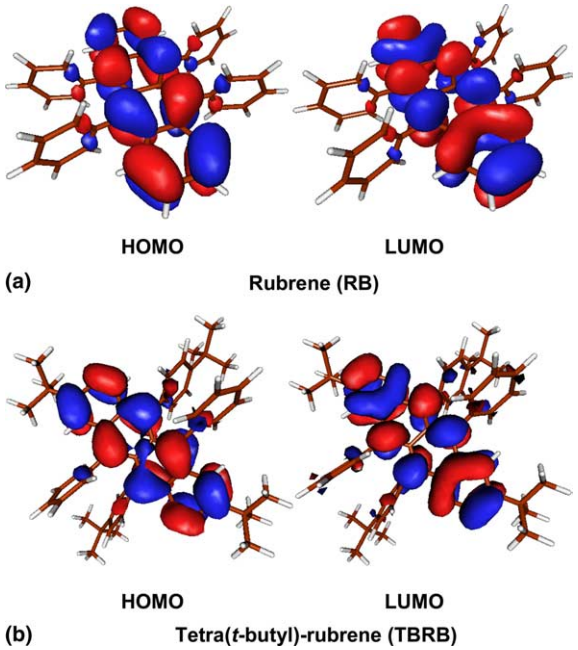

Fig. 5. The frontier orbitals of HOMO and LUMO of RB and TBRB are computed by DFT method [B3LYP/6-31G(d)] using the computed structures shown in Fig. 1(b). The contour value of the iso-surfaces is 0.02.

The origin of the energetic disorders in RB and TBRB can be examined as follows. Previous studies showed that in a molecular amorphous solid, the energetic disorder σ has two components. One component comes from van der Waals (VDW) interaction among molecules. The other originates from dipole–dipole interaction [14–17]. Based on the computed structures in Fig. 1(b), the net dipole moments of RB and TBRB can be evaluated. RB has a vanishing dipole moment whereas TBRB has a weak dipole moment of 0.16*D*. As the dipolar strength of a molecule increases, the corresponding energetic disorder in its condensed phase increases [15,16]. However, for RB and TBRB amorphous films, the dipolar contribution to the energetic disorder should be negligible as they have either zero or a weak dipole moment. Hence, the energetic disorder is dominated by the VDW component in RB or TBRB. As both molecules have similar HOMOs, their energetic disorders are expected to have similar values. Our experimental results show that RB and TBRB indeed have almost identical value energetic disorder of about 0.077 eV.

The geometric disorders are generally associated with randomness both in dipole orientations and in intermolecular separations. Given that RB and TBRB have weak dipolar interactions, the fluctuation in intermolecular separation should dominate the geometric disorder. The presence of the four *t*-butyl groups in TBRB clearly introduces additional randomness in the intermolecular separation and hence fluctuation in the hopping distances. For example, two TBRB molecules with their naphthacene moieties on top of each other would have a small hopping distance. On the other hand, the two adjacent coplanar TBRB molecules would have a much larger hopping distance due to steric effects of the *t*-butyl groups. Our observation of the increase in Σ for TBRB is consistent with the increase in the fluctuation of the hopping distances.

Our results indicate that RB and TBRB both have superior hole mobilities when compared to other common hole transporting molecules in OLEDs application [18]. For example, the hole mobility for RB is at least half an order larger than that of TPD [7]. Yet, due to the propensity of RB to form crystallites, RB is normally not used as a hole-transporting layer in an OLED. A simple means of circumventing this shortcoming in RB is to adopt a guest–host approach in which RB can be doped into an electrically inert polymeric host such as polycarbonate (PC). The electrically inert host prevents the guest molecules from aggregating. Furthermore, by adjusting the concentration of the electrically active guest molecules, one may continuously tune the conductivity of the guest–host system. This approach has been carried out previously for TPD:PC and recently for

TPD:polystyrene [19,20]. Using this concept, the hole mobility can be tuned from 10^{-7} to 10^{-3} $cm^2 V^{-1} s^{-1}$ as the concentration of TPD varies from 20% to 100% by weight [18]. With RB or TBRB as the electrically active molecules, the conductivity is expected to be tunable over a wider range because of their relatively large hole mobilities. Experiments along this direction are already underway.

4. Conclusion

The hole mobilities of amorphous RB and TBRB were measured by TOF technique. At room temperature, the hole mobility of RB is in the range of $7–9 \times 10^{-3}$ $cm^2 V^{-1} s^{-1}$ while TBRB exhibits a lower mobility of 2×10^{-3} $cm^2 V^{-1} s^{-1}$. The GDM is applicable to describe hole transport in both cases. The similarity of computed frontier HOMO orbitals in RB and TBRB is attributed to negligible electronic influence of *t*-butyl substitutions in TBRB, resulting in nearly identical energetic disorders ($\sim$0.077 eV). However, the *t*-butyl groups induce large fluctuations in the spatial separations among TBRB molecules and result in an increase in the positional disorder, and hence a reduction in hole mobility.

Acknowledgements

Support of this research by the Research Committee (FRG/01-02/II-68) of Hong Kong Baptist University and the Research Grant Council of Hong Kong under Grant HKBU/2063/00P is gratefully acknowledged. C.F.L. acknowledges partially support from the Incentive Fund of the Physics Department of the Chinese University of Hong Kong and the Information Technology Services Center (ITSC). C.H.C. also thanks the Ministry of Education of Taiwan, ROC for grant support from Program for Promoting University Academic Excellence (91-E-FA04-2-4).

References

[1] C.W. Tang, S.A. VanSlyke, C.H. Chen, J. Appl. Phys. 65 (1989) 3610.
[2] C.W. Tang, Appl. Phys. Lett. 48 (1986) 183.
[3] G. Horowitz, Adv. Mater. 10 (1998) 365.
[4] T. Fuhrmann, J. Salbeck, MRS Bull. 28 (2003) 354.
[5] Y. Hamada, H. Kanno, T. Tsujioka, H. Takahashi, T. Usuki, Appl. Phys. Lett. 75 (1999) 1682.
[6] D.J. Fatemi, H. Murata, C.D. Merritt, Z.H. Kafafi, Synth. Met. 85 (1997) 1225.
[7] H.H. Fong, K.C. Lun, S.K. So, Chem. Phys. Lett. 353 (2002) 407.
[8] V. Podzorv, V.M. Pudalov, M.E. Gershenson, Appl. Phys. Lett. 82 (2003) 1739.
[9] Y.S. Wu, T.H. Liu, C.Y. Lou, C.H. Chen, Proceedings of the International Conference on the Science and Technology of Emissive Displays and Lighting, 2002, p. 273.
[10] S.K. So, W.K. Choi, C.H. Cheung, L.M. Leung, C.F. Kwong, Appl. Phys. A 68 (1999) 447.
[11] H. Bässler, Phys. Stat. Sol. B 175 (1993) 15.
[12] A. Miller, E. Abrahams, Phys. Rev. 120 (1960) 745.
[13] M.J. Frisch, G.W. Trucks, H.B. Schlegel, G.E. Scuseria, M.A. Robb, J.R. Cheeseman, V.G. Zakrzewski, J.A. Montgomery Jr., R.E. Stratmann, J.C. Burant, S. Dapprich, J.M. Millam, A.D. Daniels, K.N. Kudin, M.C. Strain, O. Farkas, J. Tomasi, V. Barone, M. Cossi, R. Cammi, B. Mennucci, C. Pomelli, C. Adamo, S. Clifford, J. Ochterski, G.A. Petersson, P.Y. Ayala, Q. Cui, K. Morokuma, D.K. Malick, A.D. Rabuck, K. Raghavachari, J.B. Foresman, J. Cioslowski, J.V. Ortiz, A.G. Baboul, B.B. Stefanov, G. Liu, A. Liashenko, P. Piskorz, I. Komaromi, R. Gomperts, R.L. Martin, D.J. Fox, T. Keith, M.A. Al-Laham, C.Y. Peng, A. Nanayakkara, C. Gonzalez, M. Challacombe, P.M.W. Gill, B. Johnson, W. Chen, M.W. Wong, J.L. Andres, C. Gonzalez, M. Head-Gordon, E.S. Replogle, J.A. Pople, Gaussian 98, Revision A.7, Gaussian Inc., Pittsburgh PA, 1998.
[14] P.M. Borsenberger, M.B. O'Regan, Chem. Phys. 200 (1995) 257.
[15] P.M. Borsenberger, J.J. Fitzgerald, J. Phys. Chem. 97 (1993) 4815.
[16] A. Dieckmann, H. Bässler, P.M. Borsenberger, J. Chem. Phys. 99 (1993) 8136.
[17] R.H. Young, Philos. Mag. B 72 (1995) 435.
[18] P.M. Borsenberger, S.W. Weiss, Organic Photoreceptors for Imaging Systems, Marcel Dekker, New York, 1993 (Chapter 8).
[19] M. Stolka, J.F. Yanus, D.M. Pai, J. Phys. Chem. 88 (1984) 4707.
[20] J. Maldonado, M. Bishop, C. Fuentes-Hernandez, P. Caron, B. Domercq, Y. Zhang, S. Barlow, S. Thayumanavan, M. Malagoli, J. Bredas, S.R. Marder, B. Kippelen, Chem. Mater. 15 (2003) 994.